Am J Transl Res 2023;15(10):6071-6082
www.ajtr.org /ISSN:1943-8141/AJTR0151982

Original Article

Knockdown of miR-27a reduces TGFβ-induced EMT and H_2O_2-induced oxidative stress through regulating mitochondrial autophagy

Fangfang Zhao[1], Wei Wei[1], Dongping Huang[2], Yi Guo[3]

[1]*Department of Gynaecology, The First Affiliated Hospital of Guangxi Medical University, Nanning 530022, Guangxi, P. R. China;* [2]*School of Public Health, Guangxi Medical University, Nanning 530020, Guangxi, P. R. China;* [3]*Department of Clinical Laboratory, The First Affiliated Hospital of Guangxi Medical University, Nanning 530022, Guangxi, P. R. China*

Received June 29, 2023; Accepted September 22, 2023; Epub October 15, 2023; Published October 30, 2023

Abstract: Objectives: The present research aimed at clarifying the role played by miR-27a in the context of intrauterine adhesion (IUA) by focusing on its impact on TGFβ1-induced epithelial-mesenchymal transition (EMT), migration, oxidative stress, and mitochondrial autophagy in endometrial stromal cells (ESCs). Methods: We employed the Cell Counting Kit CCK-8/WST-8 assay to assess ESC proliferation, flow cytometric analysis and an Annexin-V-FITCV-FITC Apoptosis Detection kit to determine cell apoptosis, and wound healing and transwell assays to evaluate cell migration. Besides, intracellular reactive oxygen species (ROS) levels measured by the Reactive Oxygen Species Assay Kit were analyzed by flow cytometry, and protein expression levels were quantified by Western blotting analysis. Results: Knockdown of miR-27a inhibited TGFβ1-induced EMT and H_2O_2-induced oxidative stress in ESCs. H_2O_2-induced miR-27a suppressed PINK1 expression, leading to inhibition of mitophagy. MiR-27a promoted TGFβ1 or H_2O_2-induced EMT through PINK1. Conclusions: miR-27a plays a crucial role in endometrial fibrosis. It regulates TGFβ1-induced EMT, migration, oxidative stress, and apoptosis in ESCs. Additionally, miR-27a impacts mitophagy through PINK1 suppression upon H_2O_2 induction. Our findings highlight miR-27a as a potential therapeutic target for IUA treatment, shedding light on its multifaceted involvement in the mechanism of intrauterine adhesion fibrosis.

Keywords: MiR-27a, intrauterine adhesion, PINK1, EMT, oxidative stress

Introduction

Intrauterine adhesions (IUAs), or Asherman's syndrome, are characterized by the development of scar tissue within the uterus or cervix, leading to adhesions on the endometrial surface [1]. IUAs are usually caused by uterine surgery, and the main clinical manifestations include periodic abdominal pain, malpresentation, placental abruption, and abnormal pregnancy [2, 3]. Likewise, IUAs may damage the blood supply of the uterus and early fetuses [4]. It is generally accepted that IUAs are caused by endometrial basal layer damage, but there are many different claims regarding the pathogenesis of IUAs, including fibrocytosis, resulting in excessive deposition of extracellular matrix and fibrous connective tissue proliferation [5]. Endometrial fibrosis is the main pathological process of IUAs [6]. However, the precise mechanisms of IUA fibrosis remain unclear.

MicroRNAs (miRNAs), non-coding RNAs of 17-23 nucleotides, are shown to participate in a wide range of biological and pathological processes by binding to target mRNAs' 3'-UTR (3'-untranslated region), thereby inducing mRNA translational repression and degradation [7]. Recent evidence suggested the critical role played by miRNAs in fibrosis in a variety of cell types, such as pulmonary, hepatic, renal, and cardiac cells [8-10]. miR-27 has been shown to be involved in liver fibrosis in mice [11]. In addition, downregulation of miR-27a was found to be essential for angiogenesis and capillary tube formation [12]. Yet, the role played by miR-27a and the mechanisms in endometrial stromal cells (ESCs) have not been

explored. Given the role of transforming growth factor (TGF) β as a cytokine that induces endometrial fibrosis [13], TGFβ-treated ESCs are served as the *in vitro* model of IUAs [14]. Oxidative stress (OS) is closely related to the developmental process of IUA occurrence and can mediate the fibrotic process in multiple organs through mitochondria related signaling pathways [15, 16], and thus may be an important pathogenesis leading to IUA fibrosis.

Here, we investigated the role of miR-27a in TGFβ-induced epithelial mesenchymal transition (EMT) in ESCs, and further assessed its biological function in H_2O_2-induced OS. This research attempts to prove the role of miR-27a as a central regulator of EMT and OS in the context of IUAs, aiming to understand IUA pathogenesis and offer potential avenues for therapeutic development and patient care.

Materials and methods

Cell cultivation and intervention

We purchased THESCs, a telomerase-immortalized cell line, from the ATCC (American Type Culture Collection; USA) and regularly maintained them in a humidified and constant-temperature (37°C) incubator with 5% CO_2. The cells were then cultivated in Dulbecco's modified Eagle's medium (Gibco; USA) comprising 10% fetal bovine serum (Gibco; USA) and 1% penicillin-streptomycin. For TGF-β1 treatment, the transfected cells were subjected to 24 h of intervention with 15 ng/ml recombinant human TGF-β1 (ACRO Biosystems; China). For H_2O_2 treatment, cells were maintained in a medium containing 100 μM H_2O_2 for 12 h.

Transfection

All transfection procedures were performed using the Lipo 3000 transfection reagent (Thermo Fisher, USA) as per the manufacturer's instructions. The miR-27a inhibitor (5'-GAAAUCCGAUCAUCCACAGAUG-3'), mimic (5'-AGGGCUUAGCUGCUUGUGAGCACUCACAAGCAGCUAAGCCCUUU-3'), inhibitor-NC (5'-CAGUACUUUUGUGUAGUACAA-3'), and mimic-NC (5'-UUGUACUACACAAAAGUACUGGUACUUUUGUGUAGUACAAUU-3') were obtained from Sangon Biotech Shanghai. The siRNA-PINK1#1 (5'-AUAGUUCUUCAUAACGAGGAACCUCGUUAUGAAGAACUAUCC-3'), PINK1#2 (5'-UUGCUUGGGACCUCUCUUGGA CAAGAGAGGUCCCAAGCAACU-3'), PINK1#2 (5'-GAUGUUGUCGGAUUUCAGGUCCCUGAAAUCCGACAACAUCCU-3'), and siRNA-ctrl (5'-UUCUCCGAACGUGUCACGUTTACGUGACACGUUCGGAGAATT-3') were purchased from GenePharma (Shanghai, China). To overexpress PINK1, the PINK1 (CCDS211.1) coding sequence was inserted into the pCMV-Flag vector for the generation of pCMV-PINK-Flag.

Cell viability assay

Assessment of ESC proliferation was performed using the Cell Counting Kit CCK-8/WST-8 assay (Solarbio, China) as instructed by the kit manuals. Following the treatment, VSMCs were planted into the wells of a 96-well plate for 30 min incubation with the CCK-8 reagent at room-temperature. The absorbance (450 nm) of the reaction system was measured to determine the relative viability of the cells.

Flow cytometric analysis

Following the manufacturer's protocol, we determined cell apoptosis by flow cytometric analysis using an Annexin-V-FITC Apoptosis Detection kit (Solarbio, China). Viable (Annexin V+/PI-) and non-viable (Annexin V+/PI+) apoptotic ESCs were evaluated using a LSR II flow cytometer, and the obtained data were analyzed using FlowJo v10 (FlowJo, LLC).

Cell motility analysis

For the wound healing assay, cells (2×10^5) were planted into the wells of a 12-well plate for culture at 37°C. Once 100% confluence was observed, a scratch was made by scraping with a 200 μl pipette tip. The cells were then rinsed three times with serum-free medium to remove any detached cells. After incubating for 24 hours, cell observation and photographing were performed using an inverted microscope.

Matrigel (BD Bioscience, USA)-coated transwell chambers were used for cell migration assessment. In brief, transfected cells (2×10^4) cultivated in the serum-free medium were placed in the upper transwell compartment, while the bottom compartment was filled with 10% FBS-supplemented complete medium. The chambers were incubated for 24 hours in a humidified and constant-temperature environment (37°C) with 5% CO_2. After incubation, cells that remained on the upper surface of the filter were

carefully removed from the top well using Q-tips, while those migrating or invading the lower surface of the filter were treated with 70% methanol immobilization for half an hour and stained with 0.2% crystal violet.

Immunostaining

After transfection, ESCs were subjected to PBS (0.5 ml) rinsing and formaldehyde (4%) immobilization in PBS for 15 min, followed by two washes through immersing in PBT (0.5 ml; PBS + 0.1% Tween-20), blocking with BSA (5%) in Tris-buffered saline and Tween 20 (TBST) for 1 h, and overnight cultivation with primary antibody (anti-N-cadherin; 1:1,000) at 4°C. Following 2 times of 5 min TBST washes, a secondary antibody was added and incubated for 4 h at room-temperature. Nuclei were then stained with DAPI (10 μg/ml) for 5 min in PBS. Finally, a fluorescent microscope was used to photograph the immunostaining samples.

RT-qPCR

Total RNA was extracted using the TRIzol RNA isolation method (Ambion, Van Way, CA, USA), where separation was achieved by chloroform phase separation, followed by precipitation using isopropyl alcohol. The RNA pellets were then rinsed with 75% ethanol and subsequently re-dissolved in water. Reverse transcription was performed by the TaqMan MicroRNA reverse transcription kit (Life Technologies Co., Carlsbad, CA, USA) using 1 μg of RNA and random hexamers. The primer sequences (5'-3') utilized are as follows: hsa-miR-27-F: AGGGCTTAGCTGCTTGTGAG, hsa-miR-27-R: CAGTGCGTGTCGTGGAGT, homo-U6-F: CTCGCTTCGGCAGCACA, homo-U6-R: AACGCTTCACGAATTTGCGT.

Intracellular reactive oxygen species (ROS) analysis

The ROS Assay Kit (Solarbio, China) was utilized to determine intracellular ROS levels. After treatment, ESCs were rinsed using serum-free DMEM and further stained with DCFH-DA (10 μM) at 37°C for half an hour. Following suspension of the labeled ESCs in 100 μL PBS, flow cytometry was used for analysis.

Western blotting (WB) analysis

We lysed the cells using a protease and phosphatase inhibitor cocktail (Thermo Fisher Scientific, Inc.)-containing radio immunoprecipitation assay (RIPA) buffer (Solarbio, China) for 20 min on ice and then centrifuged the cells for 10 min at 12,000 g and 4°C. Protein concentration assay was then performed by using Bicinchoninic acid (BCA) protein assay kit (Beyotime Biotech, China). Protein samples of an equal amount were then isolated via 10% SDS-PAGE gel, followed by 1 h of blotting of the samples onto polyvinylidene difluoride (PVDF) membranes at 100 V on ice. After 1 h of blocking with 5% nonfat milk in TBST at room temperature, the membranes were cultivated overnight at 4°C with primary antibodies mentioned below. After 3 TBST washes, the membranes were subjected to 1 h of culture at room-temperature with the respective secondary antibodies (see below). The membranes were then incubated with ECL reagent (Millipore) to visualize proteins. Primary antibodies included β-Actin (1:3000), α-SMA (1:2000), N-cadherin (1:1500), E-cadherin (1:1500), Cytokeratins (1:2000), Bcl-2 (1:2500), Bax (1:3000), PINK1 (1:1000), Parkin (1:2000), and LC3 (1:2000). Among them, β-Actin and α-SMA antibodies were ordered from Cell Signaling Technology (Danvers, MA), and the others were from Abcam (Cambridge, UK). Secondary antibodies were all from Cell Signaling Technology (Danvers, MA), including HRP-linked anti-mouse IgG (1:8000) and HRP-linked anti-rabbit IgG (1:5000). ImageJ 1.51p was employed for quantification of immuno-blots. Alterations in protein levels were presented as normalized fold changes relative to the control.

Statistical analyses

This research used GraphPad Prism version 8.02 for statistical analyses. The results, described as mean ± standard deviation (SD), were obtained from experiments run in triplicate. Statistical comparisons were performed using ANOVA and Tukey's post hoc test, with *P*-values below 0.05 indicating statistical significance.

Results

miR-27a promoted apoptosis and inhibited proliferation of ESCs

To determine the role played by miR-27a in ESCs, we conducted gain- and loss-of-function experiments by transfecting ESCs with miR-27a

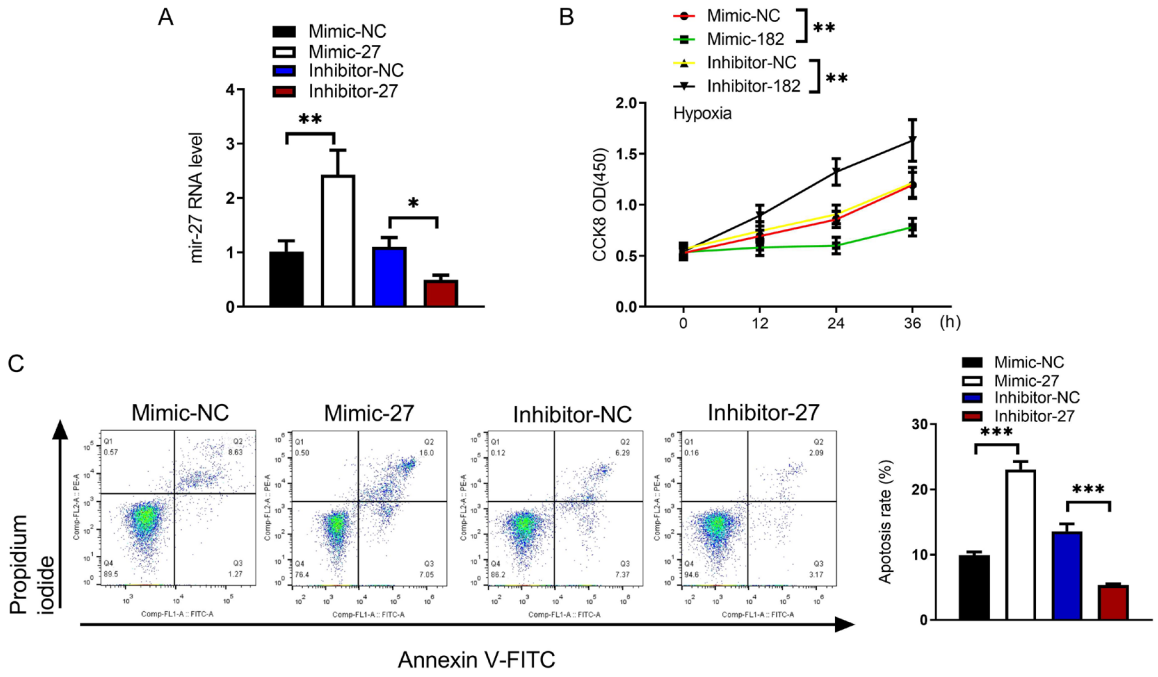

Figure 1. miR-27a mimic decreases cell proliferation and increases apoptosis in ESCs. Mimic-NC, mimic-27, inhibitor-NC, and inhibitor-27 were transfected into ESCs, respectively. A. RNA level of mir-27a was examined by qPCR. B. Cell proliferation was examined by CCK8 assay. C. Flow cytometry was carried out for cell apoptosis examination. Data were presented as mean ± SD. **P<0.01, ***P<0.001.

mimic and inhibitor, respectively. miR-27a levels were validated using RT-qPCR. miR-27a mimic transfection resulted in an upregulation of miR-27a expression, while miR-27a inhibitor transfection resulted in downregulated miR-27a levels (**Figure 1A**). According to CCK8 assay results, miR-27a overexpression could inhibit cell proliferation, whereas miR-27a knockdown promoted ESC proliferation (**Figure 1B**). Likewise, flow cytometry was carried out to evaluate the influence of miR-27a on cell apoptosis. Overexpressing miR-27a increased apoptosis rate in ESCs, whereas knocking down miR-27a produced an inverse effect (**Figure 1C**). Therefore, downregulating miR-27a expression may contribute to the survival of ESCs.

Effects of miR-27a on TGFβ1-induced EMT in ESCs

ESCs were treated with TGFβ1 (15 ng/ml) to assess the correlation of miR-27a with EMT process of ESCs. Cells from the "control" group were treated without TGFβ1 and transfections. Regarding TGFβ treatment, the pattern of cell EMT changes remained consistent between the control group and the Inhibitor negative group (Inhibitor NC) (Supplementary Figure 1). miR-27a knockdown was found to lower α-SMA and N-cadherin protein levels, and elevate Cytokeratins and E-cadherin expression in TGFβ1-treated ESCs (**Figure 2A**). The results of the wound healing assay indicated that inhibition of miR-27a weakened the migratory ability of TGFβ1-intervened ESCs (**Figure 2B**). Furthermore, consistent results were obtained from the Transwell migration assay (**Figure 2C**). Immunofluorescence staining assay results showed that knockdown of miR-27a reduced TGFβ1-induced N-cadherin expression (**Figure 2D**), indicating that miR-27a was required for TGFβ1-induced EMT in ESCs.

Knockdown of miR-27a attenuated H_2O_2-induced OS

Next, the role played by miR-27a in H_2O_2-induced OS was investigated. miR-27a expression was increased in H_2O_2-treated ESCs versus controls (**Figure 3A**). An increase of ROS production was observed in H_2O_2-treated ESCs. However, knockdown of miR-27a reduced H_2O_2-induced ROS production (**Figure 3B**). Subsequently, WB analysis demonstrated that H_2O_2 treatment led to an increase in the expression of Bax, a pro-apoptotic protein, and a decrease in Bcl-2, an anti-apoptotic protein. Knockdown of miR-27a significantly reduced

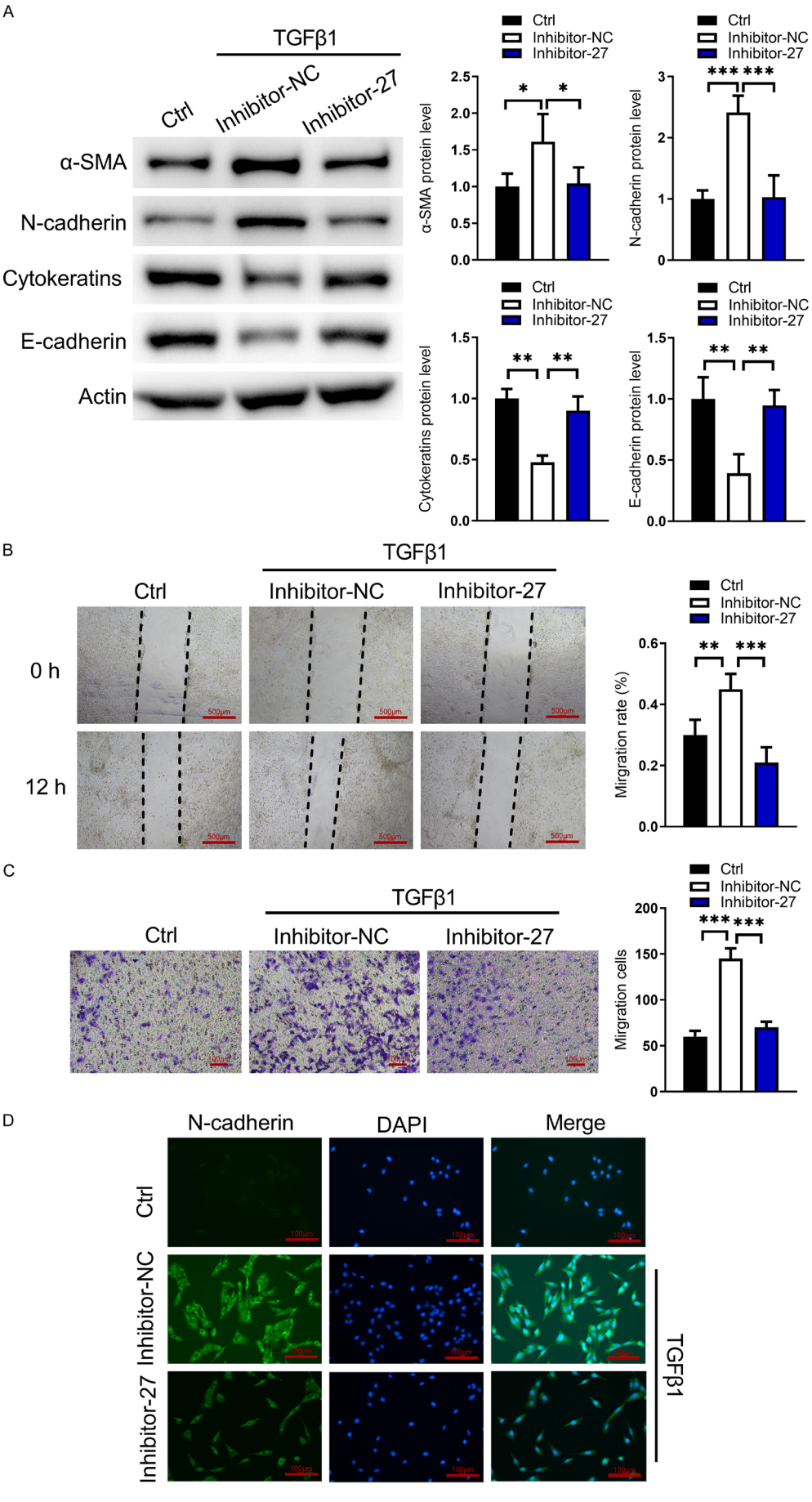
A
TGFβ1
Ctrl
Inhibitor-NC
Inhibitor-27
α-SMA
N-cadherin
Cytokeratins
E-cadherin
Actin
α-SMA protein level
N-cadherin protein level
Cytokeratins protein level
E-cadherin protein level
B
0 h
12 h
Mirgration rate (%)
C
Mirgration cells
D
N-cadherin
DAPI
Merge
Ctrl
Inhibitor-NC
Inhibitor-27
TGFβ1

Figure 2. Knockdown of miR-27a inhibits TGFβ1-induced EMT process in ESCs. ESCs, transfected with or without inhibitor-NC and inhibitor-27, were then treated with 15 ng/ml TGFβ1. (A) Western blotting was carried out to quantify α-SMA, N-cadherin, Cytokeratins, and E-cadherin protein levels. (B, C) Cell migration ability was examined by wound healing assay (B) or transwell cell migration assay (C). (D) Immunofluorescence was used to measure N-cadherin expression. Data were presented as mean ± SD. *, **, and *** represent P<0.05, P<0.01, and P<0.001, respectively.

Bax and increased Bcl-2 expression (**Figure 3C**), suggesting that knockdown of miR-27a inhibited H_2O_2-induced apoptosis. This result was further substantiated by flow cytometry analysis for apoptosis (**Figure 3D**). Moreover, miR-27a knockdown decreased phosphorylated p65 in H_2O_2-treated ESCs (**Figure 3E**). Together, these results suggested that knockdown of miR-27a attenuated H_2O_2-induced OS.

miR-27a regulated H_2O_2-induced mitophagy in ESCs by targeting PINK1

ROS has been reported to cause loss of mitochondrial membrane potential, thus activating PINK1/Parkin-dependent mitophagy [17]. We thus hypothesized the involvement of H_2O_2-induced miR-27a expression in the regulation of mitophagy through the PINK1/Parkin axis. For validation, we quantified mitochondrial autophagy-related proteins, such as PINK1, Parkin, and LC3B. Overexpressing miR-27a was found to lower PINK1 and Parkin protein levels as well as the LC3II/LC3I ratio, whereas knocking down miR-27a resulted in an inverse effect (**Figure 4A**). Treatment of ESCs with H_2O_2 resulted in a reduction of autophagy-related proteins, while miR-27a knockdown elevated the levels of these proteins. However, silencing of PINK1 blocked the effect of miR-27a knockdown (**Figure 4B**), suggesting that miR-27a exert its function through PINK1. It was also observed that miR-27a knockdown reduced H_2O_2-induced ROS production, which was markedly blocked by PINK1 silencing (**Figure 4C**). Additionally, WB results of apoptosis-associated proteins and flow cytometric assay of apoptosis yielded similar results (**Figure 4D** and **4E**). Conclusively, miR-27a regulated H_2O_2-induced mitophagy by targeting PINK1.

miR-27a modulated EMT in ESCs induced by both TGFβ and H_2O_2 through targeting PINK1

As indicated by WB analysis, overexpression of miR-27a increased α-SMA and N-cadherin expression and decreased cytokeratins and E-cadherin expression in TGFβ1-treated ESCs, while silencing of PINK1 prevented these alterations (**Figure 5A**). Transwell migration assay and wound healing assay demonstrated that miR-27a overexpression enhanced the migratory capability of TGFβ1-treated ESCs, whereas PINK1 overexpression suppressed this effect (**Figure 5B** and **5C**). Furthermore, it was also observed that H_2O_2 treatment suppressed Cytokeratins and E-cadherin protein levels, while increasing protein levels of α-SMA and N-cadherin. Treatment with miR-27a mimic further suppressed Cytokeratins and E-cadherin expression, and increased α-SMA and N-cadherin expression. However, the effects of miR-27a on these EMT markers were rescued by PINK1 overexpression in H_2O_2-treated ESCs (**Figure 5D**). Therefore, these results together suggest that miR-27a regulates EMT process in ESCs by targeting PINK1.

Discussion

IUA has shown a rapidly increasing incidence over the years, despite the availability of numerous therapies for this disorder. In-depth understanding of molecular mechanisms of IUAs is important for the prevention and development of novel treatment methods of IUA. Emerging evidence has demonstrated the critical role of miRNAs in regulating ESCs. For instance, miR-205-5p acts as a novel suppressor in endometriosis progression by targeting angiopoietin-2 (ANGPT2) [18]. Moreover, miR-26a induces ESCs apoptosis through regulating PTEN expression and PI3K/AKT pathway activation [19]. Increasing evidence has confirmed the vital clinical implications of miR-27a in drug sensitivity and cancer therapies [20]. Generally, miR-27a functions as a tumor suppressor in bladder, cervical, and breast cancers, etc. [21-23]. Yet, its function in IUAs remains elusive. In the current study, we identified miR-27a as a pivotal player in the context of IUA by influencing both TGFβ1-induced EMT and OS responses. The dual impact of miR-27a knockdown on these crucial processes underscores its multifaceted regulatory role. Distinct molecular

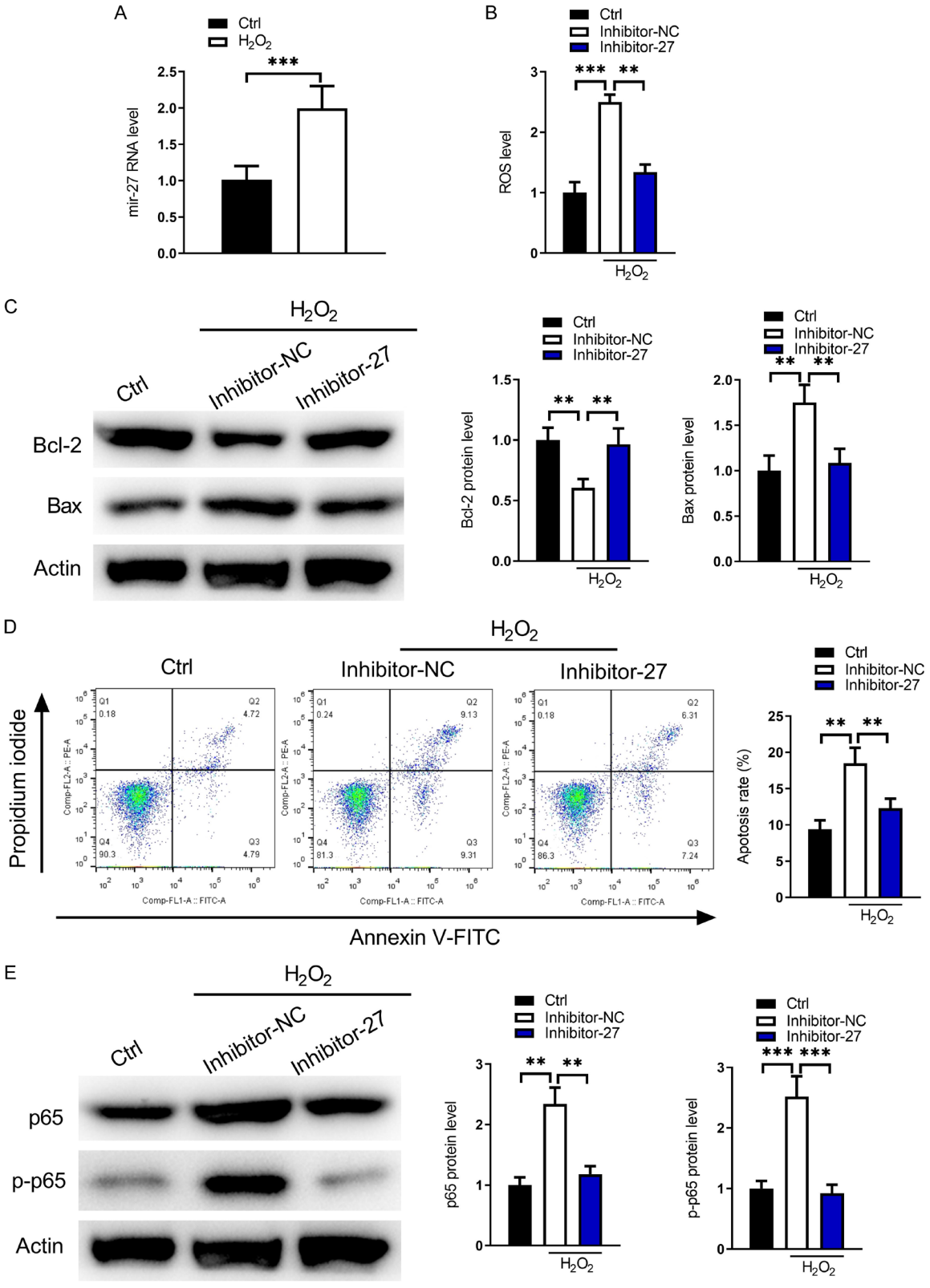

Figure 3. Downregulating miR-27a reduced H_2O_2-induced oxidative stress. A. ESCs were treated with or without H_2O_2. The miR-27a RNA level was examined by qPCR. ESCs, transfected with or without inhibitor-NC and inhibitor-27, were then intervened by 100 μM H_2O_2. B. Intracellular ROS production was detected with DCFH-DA assay. C. Western blotting was conducted to examine Bcl-2 and Bax protein levels. D. Flow cytometry was carried out for cell apoptosis examination. E. Total p65 and phosphorylated p65 levels was accessed by western blotting. Data were presented as mean ± SD. **P<0.01, ***P<0.001.

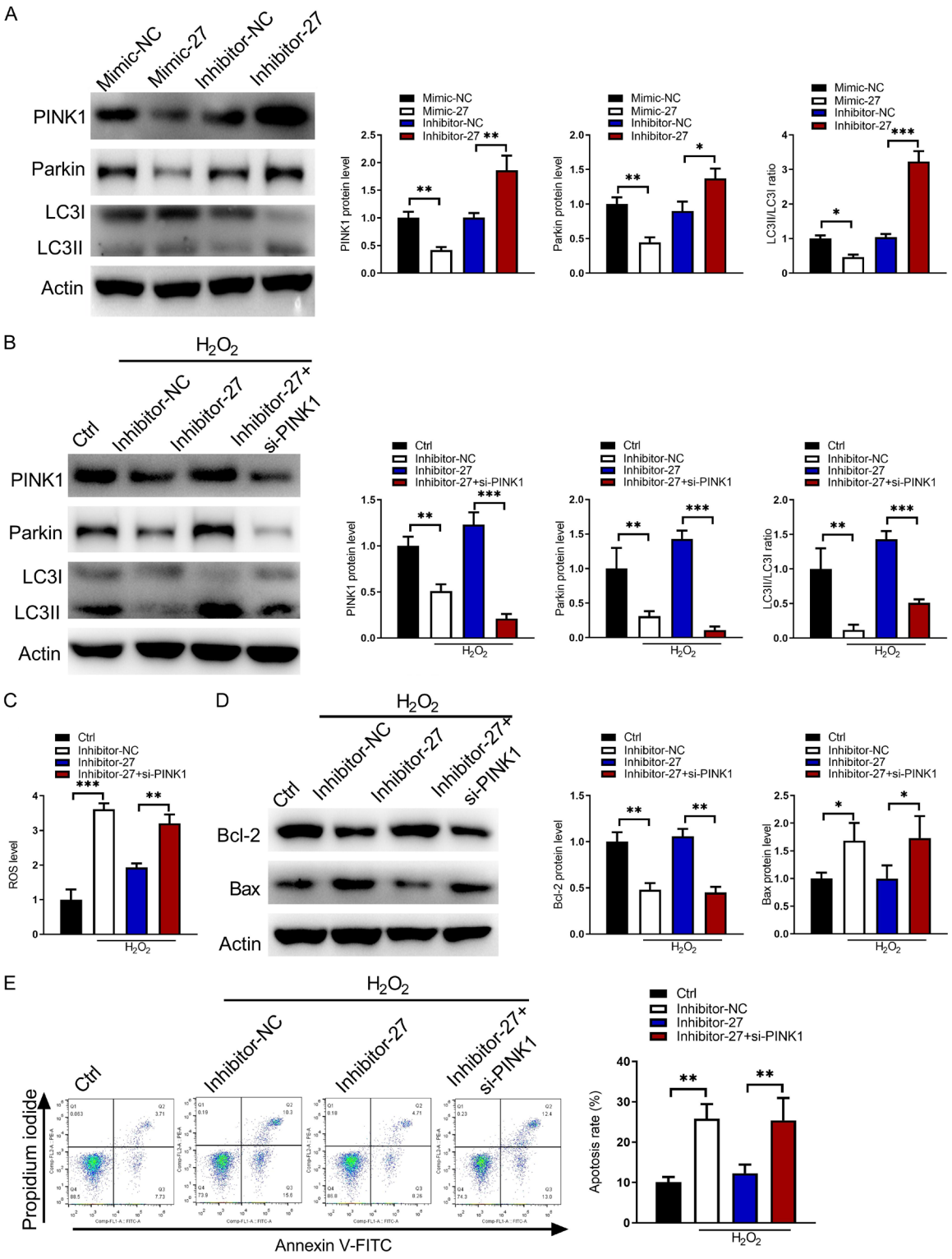

Figure 4. miR-27a regulates mitophagy in H_2O_2-treated ESCs. A. Mimic-NC, mimic-27, inhibitor-NC, and inhibitor-27 were transfected into ESCs, respectively. PINK1, Parkin, and LC3 protein levels were examined by western blotting. ESCs, transfected with inhibitor-NC, inhibitor-27, and inhibitor-27+si-PINK1, were then intervened by 100 μM H_2O_2. B. PINK1, Parkin, and LC3 protein levels were examined by western blotting. C. Intracellular ROS production was detected by DCFH-DA assay. D. Western blotting was carried out to determine Bcl-2 and Bax protein levels. E. Cell apoptosis was examined by flow cytometry. Data were presented as mean ± SD. *, **, and *** represent P<0.05, P<0.01, and P<0.001, respectively.

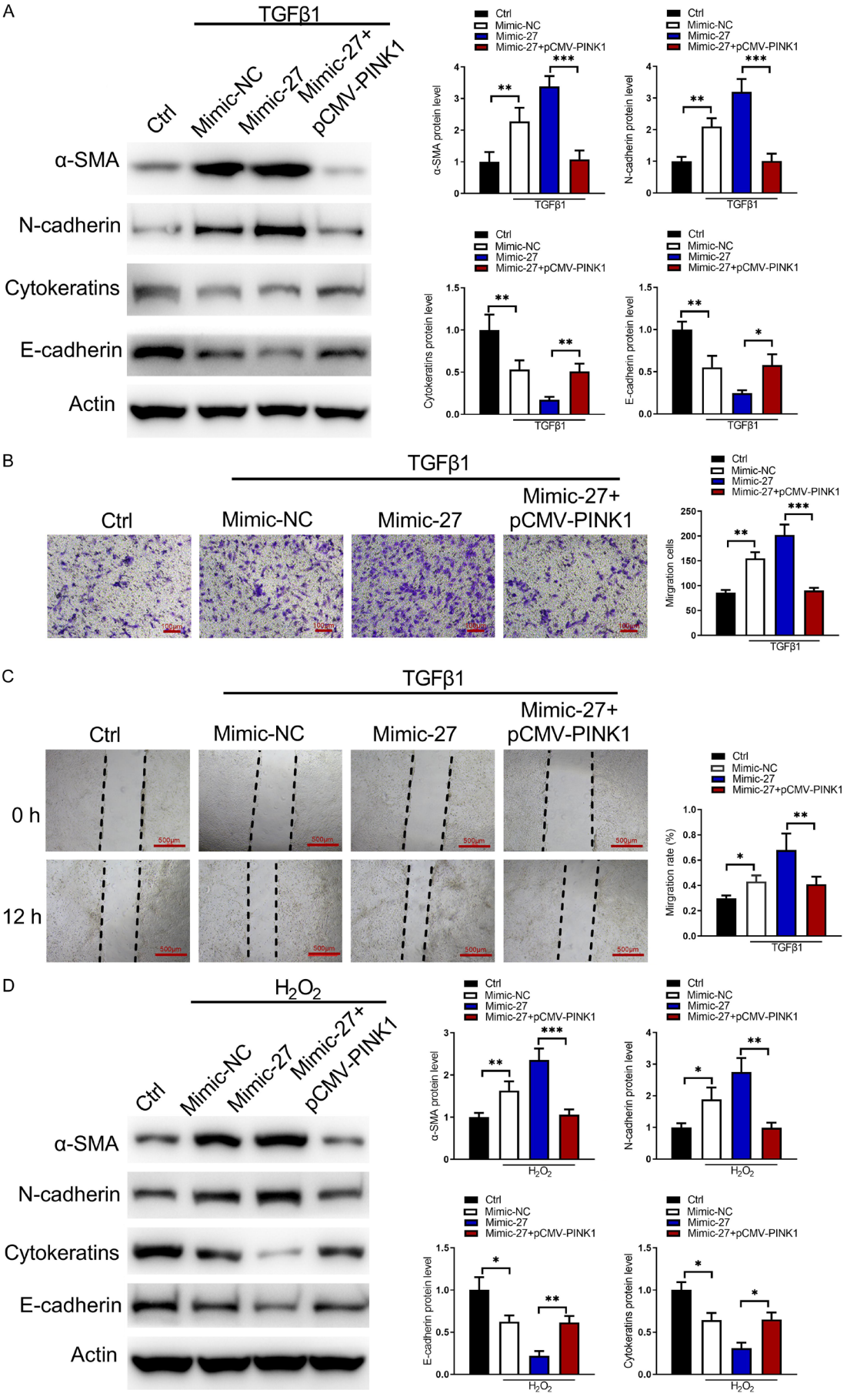
A
TGFβ1
Ctrl
Mimic-NC
Mimic-27
Mimic-27+ pCMV-PINK1
α-SMA
N-cadherin
Cytokeratins
E-cadherin
Actin
Ctrl
Mimic-NC
Mimic-27
Mimic-27+pCMV-PINK1
α-SMA protein level
N-cadherin protein level
Cytokeratins protein level
E-cadherin protein level
TGFβ1
B
TGFβ1
Ctrl
Mimic-NC
Mimic-27
Mimic-27+ pCMV-PINK1
Migration cells
C
TGFβ1
Ctrl
Mimic-NC
Mimic-27
Mimic-27+ pCMV-PINK1
0 h
12 h
Migration rate (%)
D
H2O2
Ctrl
Mimic-NC
Mimic-27
Mimic-27+ pCMV-PINK1
α-SMA
N-cadherin
Cytokeratins
E-cadherin
Actin
α-SMA protein level
N-cadherin protein level
E-cadherin protein level
Cytokeratins protein level
H2O2

Figure 5. miR-27a promotes TGFβ1-induced EMT process via PINK1. ESCs, transfected with mimic-NC, mimic-27, and mimic-27+pCMV-PINK1, were then intervened by 15 ng/ml TGFβ1. (A) Protein levels of α-SMA, N-cadherin, Cytokeratins, and E-cadherin were examined by western blotting. (B, C) Cell migration capacity was examined by transwell assay (B) or wound healing assay (C). (D) ESCs, transfected with mimic-NC, mimic-27, and mimic-27+pCMV-PINK1, were then subjected to 100 μM H_2O_2 treatment. Protein levels of α-SMA, N-cadherin, Cytokeratins, and E-cadherin were examined by western blotting. Data were presented as mean ± SD. *P<0.05, **P<0.01, ***P<0.001.

mechanisms underlying miR-27a's involvement in EMT have been delineated across various cell models. In lung epithelial cells, miR-27a suppressed EMT via a regulation of Smad3 expression [24]. Conversely, in ovarian cancer, miR-27a facilitated EMT by targeting FOXO1 [25]. Numerous studies have linked OS to the occurrence and progression of gynecological diseases, such as recurrent pregnancy loss, endometriosis, and infertility [26]. Oxidative stress is caused by excessive production of intracellular ROS, which is crucial conspirators in EMT engagement [27]. NF-κB, a critical nuclear transcription factor in cells, participates in many physiological processes such as OS, inflammation, and cytokine stimulation [28]. Increased levels of intracellular ROS lead to NF-κB activation, causing its translocation into the nucleus to initiate a transcriptional program of a series of downstream target genes. NF-κB levels have also been shown to be obviously upregulated in endometrial tissues of IUA patients and correlated with the degree of uterine adhesions, indicating the involvement of NF-κB signaling in uterine fibrosis progression in IUA [15]. Here, we observed reduced ROS production and NF-κB activation when miR-27a was knocked down, leading to inhibition of H_2O_2-induced apoptosis (**Figure 3**). Interestingly, a prior investigation has unveiled that miR-27b curtailed NF-κB activation in lipopolysaccharide-treated RAW 264.7 cells. This suggests that under varying stimuli, all miR-27 family genes can impede the NF-κB pathway activation [29].

Mitophagy is an important mechanism by which cells maintain redox balance by clearing damaged mitochondria thereby limiting ROS overaccumulation and preventing potential oxidative damage to cells [30]. However, the mechanisms by which mitophagy regulates endometrial fibrosis remain unclear. Mitochondrial autophagy involves multiple signaling pathways, and PINK1/Parkin pathway plays an important role in organ fibrosis diseases [31]. Previously, miR-27a and miR-27b were reported to translationally reduce PINK1 expression through direct binding to its mRNA 3'UTR, resulting in inhibition of mitophagic influx [32]. We found that knockdown of miR-27a promoted mitophagy via PINK1 in H_2O_2-treated ESCs (**Figure 4**). Recent studies have shown that PINK1-dependent mitophagy is closely correlated with TLR9 and NF-κB activation [33]. Thus, it is possible that H_2O_2-induced miR-27a suppressed mitophagy and hence NF-κB activation. PINK1 has been shown to be involved in TGFβ1-induced fibrosis. For example, Avignat et al. reported that PINK1 ameliorated cell death and inhibited TGFβ1-induced fibrogenesis in pulmonary fibrosis [34]. Our findings elucidated that the augmentation of PINK1 hindered the actions of miR-27a, underscoring its role in fostering EMT and migration through PINK1 in TGFβ1-treated ESCs (**Figure 5**). Indeed, in addition to TGFβ1, H_2O_2 treatment also can induce EMT [35]. Furthermore, H_2O_2-producing NADPH oxidase contributed to the invasive behaviors of tumors and/or the EMT in cancer [36]. Elevated miR-27a expression heightened N-cadherin levels while reducing E-cadherin expression. However, this effect was counteracted upon PINK1 overexpression. These observations underscore that miR-27a modulates the expression of EMT-associated proteins via PINK1 in H_2O_2-treated ESCs. Conclusively, this study revealed the biological role of miR-27a in ESCs and the regulation mechanism. Our results provided evidence that the suppression of miR-27a not only mitigated H_2O_2-induced apoptosis but also bolstered mitophagy, and these effects were mediated through PINK1. In addition, knockdown of miR-27a suppressed EMT and migration of TGFβ1-treated ESCs by PINK1. Our results provide a basis for further understanding the mechanism of miRNAs in endometrial fibrosis. However, there are certain limitations in this study. The study primarily focuses on ESCs, which might not fully capture the complexity of the intrauterine environment. Incorporating additional cell types or *in vivo* models could enhance the relevance and translat-

ability of the findings. While the study highlights the significant role of miR-27a, other regulatory factors contributing to IUA may also be at play. Exploring a broader range of miRNAs or molecular pathways could provide a more comprehensive understanding. In conclusion, while this study presents significant findings regarding miR-27a's role in ESCs, acknowledging its limitations and capitalizing on its prospective implications will pave the way for future advancements in both scientific knowledge and clinical practice.

Disclosure of conflict of interest

None.

Address correspondence to: Fangfang Zhao, Department of Gynaecology, The First Affiliated Hospital of Guangxi Medical University, Nanning 530022, Guangxi, P. R. China. Tel: +86-0771-5356593; E-mail: zff1975@163.com

References

[1] March CM. Asherman's syndrome. Semin Reprod Med 2011; 29: 83-94.

[2] Bosteels J, Weyers S, Mol BW and D'Hooghe T. Anti-adhesion barrier gels following operative hysteroscopy for treating female infertility: a systematic review and meta-analysis. Gynecol Surg 2014; 11: 113-127.

[3] Xiao S, Wan Y, Xue M, Zeng X, Xiao F, Xu D, Yang X, Zhang P, Sheng W, Xu J and Zhou S. Etiology, treatment, and reproductive prognosis of women with moderate-to-severe intrauterine adhesions. Int J Gynaecol Obstet 2014; 125: 121-124.

[4] Taylor PJ, Cumming DC and Hill PJ. Significance of intrauterine adhesions detected hysteroscopically in eumenorrheic infertile women and role of antecedent curettage in their formation. Am J Obstet Gynecol 1981; 139: 239-242.

[5] Chinese Society of Obstetrics and Gyneocology; Chinese Medical Association. Expert consensus on the diagnosis and management of intrauterine adhesions in China. Zhonghua Fu Chan Ke Za Zhi 2015; 50: 881-887.

[6] Bai X, Liu J, Cao S and Wang L. Mechanisms of endometrial fibrosis and the potential application of stem cell therapy. Discov Med 2019; 27: 267-279.

[7] Bartel DP. MicroRNAs: genomics, biogenesis, mechanism, and function. Cell 2004; 116: 281-297.

[8] Wu K, Ye C, Lin L, Chu Y, Ji M, Dai W, Zeng X and Lin Y. Inhibiting miR-21 attenuates experimental hepatic fibrosis by suppressing both the ERK1 pathway in HSC and hepatocyte EMT. Clin Sci (Lond) 2016; 130: 1469-1480.

[9] Bijkerk R, de Bruin RG, van Solingen C, van Gils JM, Duijs JM, van der Veer EP, Rabelink TJ, Humphreys BD and van Zonneveld AJ. Silencing of microRNA-132 reduces renal fibrosis by selectively inhibiting myofibroblast proliferation. Kidney Int 2016; 89: 1268-1280.

[10] Mo Y, Zhang Y, Wan R, Jiang M, Xu Y and Zhang Q. miR-21 mediates nickel nanoparticle-induced pulmonary injury and fibrosis. Nanotoxicology 2020; 14: 1175-1197.

[11] Rogler CE, Matarlo JS, Kosmyna B, Fulop D and Rogler LE. Knockdown of miR-23, miR-27, and miR-24 alters fetal liver development and blocks fibrosis in mice. Gene Expr 2017; 17: 99-114.

[12] Young JA, Ting KK, Li J, Moller T, Dunn L, Lu Y, Moses J, Prado-Lourenco L, Khachigian LM, Ng M, Gregory PA, Goodall GJ, Tsykin A, Lichtenstein I, Hahn CN, Tran N, Shackel N, Kench JG, McCaughan G, Vadas MA and Gamble JR. Regulation of vascular leak and recovery from ischemic injury by general and VE-cadherin-restricted miRNA antagonists of miR-27. Blood 2013; 122: 2911-2919.

[13] Bai X, Liu J, Yuan W, Liu Y, Li W, Cao S, Yu L and Wang L. Therapeutic effect of human amniotic epithelial cells in rat models of intrauterine adhesions. Cell Transplant 2020; 29: 963689720908495.

[14] Ai Y, Chen M, Liu J, Ren L, Yan X and Feng Y. lncRNA TUG1 promotes endometrial fibrosis and inflammation by sponging miR-590-5p to regulate Fasl in intrauterine adhesions. Int Immunopharmacol 2020; 86: 106703.

[15] Wu B, Chen X, He B, Liu S, Li Y, Wang Q, Gao H, Wang S, Liu J, Zhang S, Xu X and Wang J. ROS are critical for endometrial breakdown via NF-kappaB-COX-2 signaling in a female mouse menstrual-like model. Endocrinology 2014; 155: 3638-3648.

[16] Wang J, Shen W, Zhang JY, Jia CH and Xie ML. Stevioside attenuates isoproterenol-induced mouse myocardial fibrosis through inhibition of the myocardial NF-kappaB/TGF-beta1/Smad signaling pathway. Food Funct 2019; 10: 1179-1190.

[17] Wang Y, Nartiss Y, Steipe B, McQuibban GA and Kim PK. ROS-induced mitochondrial depolarization initiates PARK2/PARKIN-dependent mitochondrial degradation by autophagy. Autophagy 2012; 8: 1462-1476.

[18] Zhou CF, Liu MJ, Wang W, Wu S, Huang YX, Chen GB, Liu LM, Peng DX, Wang XF, Cai XZ, Li XX, Feng WQ and Ma Y. miR-205-5p inhibits human endometriosis progression by targeting

ANGPT2 in endometrial stromal cells. Stem Cell Res Ther 2019; 10: 287.
[19] Zhang L, Liu X, Liu J, Ma X, Zhou Z, Song Y and Cao B. miR-26a promoted endometrial epithelium cells (EECs) proliferation and induced stromal cells (ESCs) apoptosis via the PTEN-PI3K/AKT pathway in dairy goats. J Cell Physiol 2018; 233: 4688-4706.
[20] Li X, Xu M, Ding L and Tang J. MiR-27a: a novel biomarker and potential therapeutic target in tumors. J Cancer 2019; 10: 2836-2848.
[21] Li X, Liu X, Xu W, Zhou P, Gao P, Jiang S, Lobie PE and Zhu T. c-MYC-regulated miR-23a/24-2/27a cluster promotes mammary carcinoma cell invasion and hepatic metastasis by targeting Sprouty2. J Biol Chem 2013; 288: 18121-18133.
[22] Sun Y, Yang X, Liu M and Tang H. B4GALT3 upregulation by miR-27a contributes to the oncogenic activity in human cervical cancer cells. Cancer Lett 2016; 375: 284-292.
[23] Drayton RM, Dudziec E, Peter S, Bertz S, Hartmann A, Bryant HE and Catto JW. Reduced expression of miRNA-27a modulates cisplatin resistance in bladder cancer by targeting the cystine/glutamate exchanger SLC7A11. Clin Cancer Res 2014; 20: 1990-2000.
[24] Dong M, Wang X, Guan Y and Li T. MiR-27a-3p downregulation contributes to the development of occlusive bronchiolitis. Cell Stress Chaperones 2019; 24: 883-889.
[25] Zhang LY, Chen Y, Jia J, Zhu X, He Y and Wu LM. MiR-27a promotes EMT in ovarian cancer through active Wnt/β-catenin signalling by targeting FOXO1. Cancer Biomark 2019; 24: 31-42.
[26] Da Broi MG and Navarro PA. Oxidative stress and oocyte quality: ethiopathogenic mechanisms of minimal/mild endometriosis-related infertility. Cell Tissue Res 2016; 364: 1-7.
[27] Giannoni E, Parri M and Chiarugi P. EMT and oxidative stress: a bidirectional interplay affecting tumor malignancy. Antioxid Redox Signal 2012; 16: 1248-1263.
[28] Reale C, Zotti T, Scudiero I, Vito P and Stilo R. The NF-kappaB family of transcription factors and its role in thyroid physiology. Vitam Horm 2018; 106: 195-210.
[29] Thulasingam S, Massilamany C, Gangaplara A, Dai H, Yarbaeva S, Subramaniam S, Riethoven JJ, Eudy J, Lou M and Reddy J. miR-27b*, an oxidative stress-responsive microRNA modulates nuclear factor-kB pathway in RAW 264.7 cells. Mol Cell Biochem 2011; 352: 181-188.
[30] Filomeni G, De Zio D and Cecconi F. Oxidative stress and autophagy: the clash between damage and metabolic needs. Cell Death Differ 2015; 22: 377-388.
[31] Kang JW, Hong JM and Lee SM. Melatonin enhances mitophagy and mitochondrial biogenesis in rats with carbon tetrachloride-induced liver fibrosis. J Pineal Res 2016; 60: 383-393.
[32] Kim J, Fiesel FC, Belmonte KC, Hudec R, Wang WX, Kim C, Nelson PT, Springer W and Kim J. miR-27a and miR-27b regulate autophagic clearance of damaged mitochondria by targeting PTEN-induced putative kinase 1 (PINK1). Mol Neurodegener 2016; 11: 55.
[33] Jing R, Hu ZK, Lin F, He S, Zhang SS, Ge WY, Dai HJ, Du XK, Lin JY and Pan LH. Mitophagy-mediated mtDNA release aggravates stretching-induced inflammation and lung epithelial cell injury via the TLR9/MyD88/NF-kappaB pathway. Front Cell Dev Biol 2020; 8: 819.
[34] Patel AS, Song JW, Chu SG, Mizumura K, Osorio JC, Shi Y, El-Chemaly S, Lee CG, Rosas IO, Elias JA, Choi AM and Morse D. Epithelial cell mitochondrial dysfunction and PINK1 are induced by transforming growth factor-beta1 in pulmonary fibrosis. PLoS One 2015; 10: e0121246.
[35] Lee HB and Ha H. Mechanisms of epithelial-mesenchymal transition of peritoneal mesothelial cells during peritoneal dialysis. J Korean Med Sci 2007; 22: 943-945.
[36] Meitzler JL, Konate MM and Doroshow JH. Hydrogen peroxide-producing NADPH oxidases and the promotion of migratory phenotypes in cancer. Arch Biochem Biophys 2019; 675: 108076.

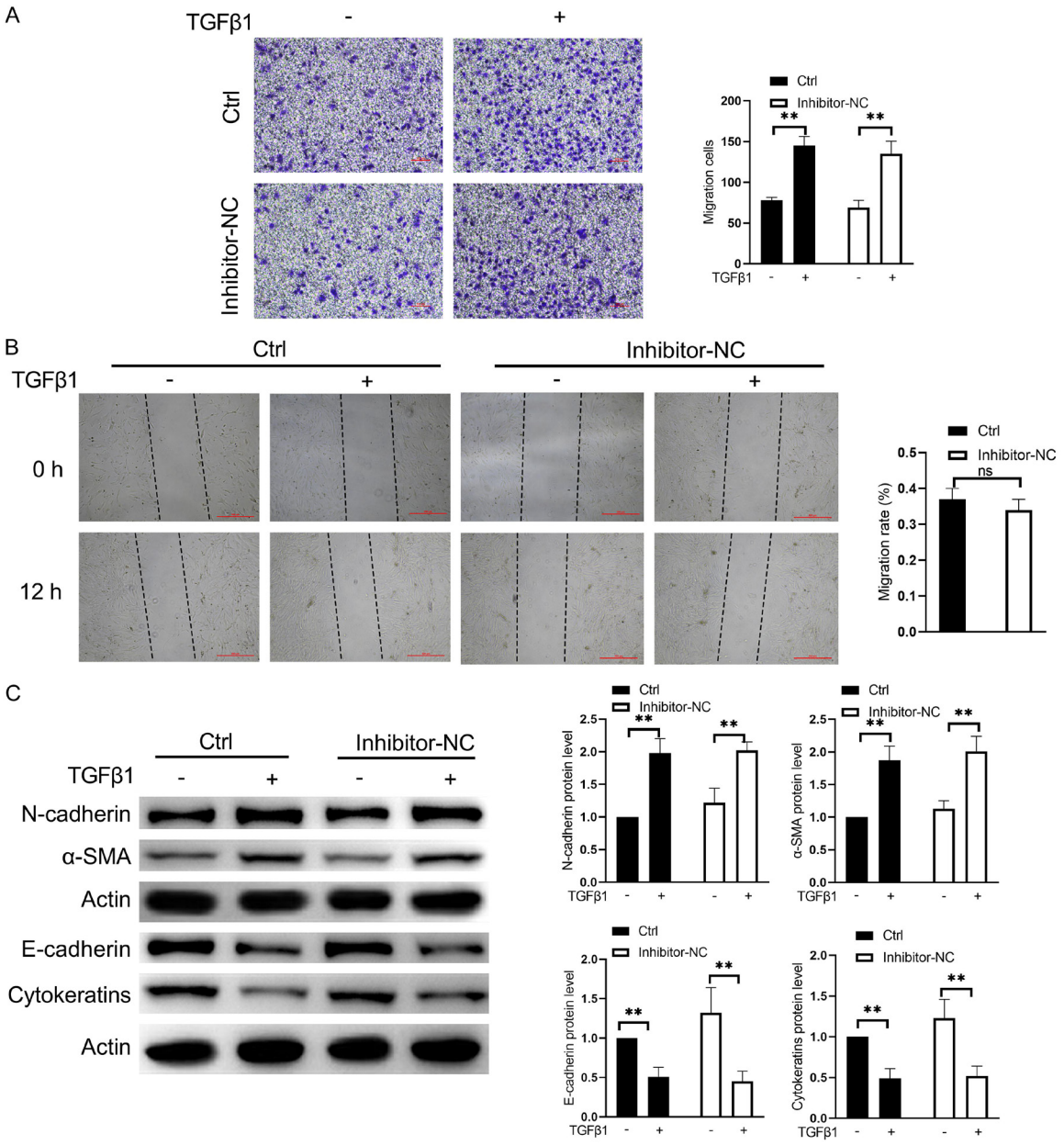

Supplementary Figure 1. ESCs were transfected with or without inhibitor-NC. (A, B) Cell migration ability was examined by transwell (A) or wound healing assay (B). (C) Western blotting was carried out to quantify α-SMA, N-cadherin, Cytokeratins, and E-cadherin protein levels. Data were presented as mean ± SD. **P<0.01; ns-no significant difference.